

STUDIES OF A MIXED ADSORPTION LAYER OF *n*-BUTANOL AND *m*- AND *p*-TOLUIDINE ON MERCURY ELECTRODE

Jadwiga SABA

*Faculty of Chemistry,**M. Curie-Skłodowska University, 20031 Lublin, Poland*

Received September 14, 1994

Accepted June 5, 1995

The mixed adsorption layers of *n*-butanol-*m*-toluidine and *n*-butanol-*p*-toluidine were studied and the surface excess of pure components and their mixtures was determined. The occurrence of synergetic coadsorption was observed. The rate constants of Zn(II) ion reduction were determined in 1 mol l^{-1} NaClO_4 in presence of *n*-butanol as an inhibitor, *m*- and *p*-toluidine as accelerating substances and in their mixtures. It was found that the inhibiting or accelerating effect depends on the concentration of *n*-butanol and *m*- or *p*-toluidine. Compensation of these effects achieved at the concentration ratio of $C_{\text{BU}} : C_{\text{pT}} \approx 35$ and $C_{\text{BU}} : C_{\text{mT}} \approx 85$ in a wide concentration range is an evidence of toluidine predominance in the formation of a mixed adsorption layer.

The effects of coadsorption of different organic substances on the electrode provide useful informations for the studies of metal electrodeposition and corrosion protection. The survey of papers on mixed adsorption on the mercury electrode reveals following trends:

– Adsorption of two organic, electroinactive substances possessing character of typical inhibitors of electrode processes, represented by the systems of tetramethylammonium cation and nonyl sulfate anion in $0.5 \text{ M Na}_2\text{SO}_4$ (ref.¹) two aliphatic alcohols or aliphatic alcohol and valeric acid², β -naphthol and tetramethylammonium cation³. Based on the adsorption studies, it was stated that the constants characterizing interactions between the adsorbed molecules are higher than those for individual substances. An exception is the coadsorption of two aliphatic alcohols due to the similarity of their structures.

– Adsorption of two organic substances with one of them electroactive, such as methylene blue and Triton X-100. Reduction of methylene blue studied by the voltammetry in presence of Triton X-100 takes place at potentials by about 160 mV more positive than in its absence. It is explained by a dissolution of methylene blue in the aliphatic subphase of Triton adsorbed on the electrode⁴. In turn, cephalosporin reduction is inhibited in the presence of Triton X-100. In the case of large surface coverage an inhibition mechanism based on the model of competitive adsorption was assumed. From the dependence of the rate constant on the logarithm of surfactant concentration,

it is possible to calculate the ratio of the number of molecules displaced from the electrode surface by the reagent to that displaced by surfactant⁵.

– Adsorption of two organic, electroinactive substances possessing an inhibitor character, studied indirectly by means of the electroreduction of chosen ion in the model system dodecylsodium sulfate–dodecyl alcohol and Cd(II) ion. The differential capacity of the double layer in the mixture of both substances at the potential of maximum adsorption is higher than that for individual substances. The change from inhibition to acceleration at relatively high concentrations of surfactants indicates an increase of permeability of the mixed adsorption layer for Cd(II) ions⁶.

– Adsorption of two organic electroinactive substances with one of them as an inhibitor and the other as an accelerator of metal ion electroreduction according to the cap-pair rule^{7,8}, which determines the conditions to be met by an accelerator.

The systems of couples inhibitor–accelerator such as tween 80–thiourea⁹, detergents–thiourea or detergents–diaminotoluene¹⁰, polyglycols–thiourea¹¹, n-butanol–thiourea¹², benzo-15-crown-5–thiourea¹³ were studied with respect to adsorption and kinetics of Zn(II) or Cd(II) electroreduction. By a change of relative concentrations of components in the mixture, the systems display inhibiting, neutral or accelerating effects on the electrochemical reduction. This is a source of informations about layers formed by a mixed adsorption.

The paper brings the results of study on the layers formed by a mixed adsorption of n-butanol (BU) and *m*- and *p*-toluidine isomers on the mercury electrode in 1 M NaClO₄. The reduction of piloting Zn(II) ion is accelerated by *m*-toluidine (mT) and *p*-toluidine (pT) and inhibited by BU. An inhibitor was chosen because of its well known adsorption behavior on the mercury electrode^{14–16}.

EXPERIMENTAL

Technique of Measurement

Polarographic measurements were carried out using a PA-4 polarograph (Laboratorni pristroje) or a polarographic analyzer model 384B (EG & G PARC). The static mercury dropping electrode (SMDE) with the drop surface of 0.01434 cm² (Laboratorni pristroje) or model 303A (EG & G PARC) were employed as working electrodes. A saturated (NaCl) calomel electrode or Ag/AgCl electrode served as reference electrodes. The potential difference between SCE prepared from NaCl and KCl was about –5 mV.

A platinum wire was used as an auxiliary electrode. The reference electrode was connected to the cell via a salt bridge filled with the cell solution. All potentials are referred to the SCE. The differential capacity of the double layer was calculated from the data obtained at the frequency of 800 Hz using an impedance meter EIM-2 (manufactured by the Lodz University). The flow-rate of mercury was determined to $9.45 \cdot 10^{-4} \text{ g s}^{-1}$ at the height of the mercury column of 50 cm. The reproducibility of the capacity measurements was about $\pm 1\%$ over a wide range of potentials. For the whole polarization range the capacity dispersion was tested at five different frequencies between 200–2 000 Hz. In the potential range studies, no dispersion of the capacitance was observed. The potential of zero

charge (PZC) was measured for each solution using the streaming mercury electrode. Interfacial tension at PZC was measured by the maximum bubble pressure following Schiffrin's method¹⁷.

Cell impedances and cyclic chronovoltammetric curves were measured using Model 388 and 270 Electrochemical Impedance and Analysis System (EG & G PARC). The complex cell impedance was obtained at 18 frequencies between 100 Hz and 20 kHz within faradaic region at the formal potential. Measurements were performed at 25 ± 0.1 °C. All solutions were prepared from analytical grade chemicals (Merck) and fresh double distilled water, deoxygenated by high-purity nitrogen purified using vanadium(II) sulfate solution; $\text{Zn}(\text{NO}_3)_2 \cdot 6 \text{H}_2\text{O}$ was used without further purification, mercury was purified and double distilled.

Elaboration of Experimental Data

Measurements of differential capacity were carried out in $1 \text{ mol l}^{-1} \text{ NaClO}_4$ solution, pH 3, with concentrations of BU ranging from 0.11 to 0.55 mol l^{-1} , mT or pT from 0.0015 to 0.05 mol l^{-1} . The surface excess Γ at the constant charge σ was determined using the equation (1)

$$\Gamma = -(1/RT) (d\xi/d \ln C_{\text{org}})\sigma, \quad (1)$$

where C_{org} is the concentration of mT, pT, BU or toluidine in the solution mixture of mT and BU or pT and BU at the constant concentration of BU if constant ionic strength is supposed; ξ is the Parsons function¹⁸ $\xi = \gamma + \sigma E$.

The rectilinear dependence of the electrode potential on Γ at constant charge confirms congruence of the obtained isotherms.

The approximate diffusion coefficients of Zn(II) were calculated using Ilkovic equation for diffusion-controlled limiting current¹⁹. The polarographic wave of Zn(II) in $0.1 \text{ mol l}^{-1} \text{ KNO}_3$ with the value of the Zn(II) diffusion coefficient of $6.9 \cdot 10^{-6} \text{ cm}^2 \text{ s}^{-1}$ (ref.²⁰) was used as a standard. The diffusion coefficient of Zn(II) ions in $1 \text{ mol l}^{-1} \text{ NaClO}_4$ was found to be $6.6 \cdot 10^{-6} \text{ cm}^2 \text{ s}^{-1}$ at 25 °C. The diffusion coefficient of zinc in mercury having value of $1.67 \cdot 10^{-5} \text{ cm}^2 \text{ s}^{-1}$ was taken from literature²¹, all of them with the accuracy of $\pm 5\%$.

The formal potentials E_0^f of the reduction of Zn(II) were estimated from cyclic voltammetric curves²² at sweep rates from 5 to 20 mV s^{-1} with the accuracy of $\pm 2 \text{ mV}$. The formal potential E_0^f of Zn(II) ions in $1 \text{ mol l}^{-1} \text{ NaClO}_4$ was found to be -0.991 V .

The ohmic resistance of the electrolyte solution was obtained as a real impedance component at a frequency of 10 kHz and at a potential outside the faradaic region. The activation polarization resistances R_A were determined for E_0^f and calculated from the dependence $Z' = f(\omega Z'')$ or $Z'' = f(Z')$ (refs^{23,24}) where Z' is the real and Z'' the imaginary parts of the cell impedance. The reaction rate constants k_s were calculated according to the expression (2)

$$k_s = \frac{RT}{n^2 F^2 c R_A}, \quad (2)$$

where $c = 5 \cdot 10^{-3} \text{ mol l}^{-1}$ is the concentration of depolarizer.

RESULTS AND DISCUSSION

Polarographic Measurements

Polarograms of differential pulse polarography (DPP) and square wave voltammetry (SWV) for Zn(II) ions in the presence of toluidine isomers indicate a significant increase of the peak current up to $5 \cdot 10^{-3}$ mol l⁻¹ toluidine. At the higher toluidine concentrations a plateau is reached. The choice of toluidine maximum concentration of 0.05 mol l⁻¹ was given by its solubility. The values of peak currents indicate a greater accelerating effect of pT compared to mT, particularly at lower concentrations. In the presence of BU, the peak current of Zn(II) reduction decreases monotonically with the increase of BU concentration. The corresponding peak potentials are shifted towards positive values with the increase of toluidine isomers concentration by +30 mV at maximum. In the presence of BU the direction of potential shift is reversed to -90 mV at maximum.

Peak potentials and peak currents of Zn(II) reductions in BU and toluidine isomers mixtures show intermediate values compared with those obtained for individual substances. At a relatively higher toluidine/BU concentration ratio, an increase of the zinc peak is observed compared with the values obtained in pure 1 mol l⁻¹ NaClO₄.

Adsorption of Toluidine Isomers, BU and Their Mixtures

On the curves of differential capacity obtained for different concentrations of *m*- and *p*-toluidine in 1 mol l⁻¹ NaClO₄ well defined desorption peak is observed. Its potential is shifted from -1.00 V to -1.35 V in presence of pT and from -1.05 V to -1.35 V for mT with rising toluidine concentration. At toluidine concentrations below 0.01 mol l⁻¹ higher differential capacity is observed in the whole potential range from -0.2 V to -1.6 V compared to pure NaClO₄ solution. For higher toluidine concentrations, however, a significant drop in a differential capacity was observed. For the maximum pT concentration of 0.05 mol l⁻¹ this drop was found in the potential range from -0.5 V to -1.1 V. For mT the differential capacity showed its minimum in the potential range from -0.5 V to -1.2 V.

In the case of BU adsorption a significant decrease of the differential capacity takes place in wider potential range compared with the supporting electrolyte. This range becomes broader with an increase of BU concentration. For the concentration of 0.55 mol l⁻¹ it extends from -0.22 V to -1.2 V. On these curves a well defined desorption peak appears with the peak potential shifted from -1.05 V to -1.35 V with an increase of BU concentration.

Figures 1 and 2 represent the differential capacity curves of 0.008 mol l⁻¹ pT and mT mixture depending on BU concentration. The potential range, at which a differential capacity drop takes place, depends on the BU/toluidine concentration ratio. For a given

concentration of pT or mT the potential range in which the differential capacity drop takes place is broadened with increasing BU concentration.

Table I presents the values of potentials of zero charge (PZC) for the solutions containing pT, mT, BU and their mixture. Concentration increase of BU causes a significant shift of the PZC towards positive potentials. An addition of pT or mT into 1 mol l^{-1} NaClO_4 causes at first a distinct shift of the PZC towards negative potentials. Further

TABLE I

Potential of zero charge (PZC in mV vs SCE) for pT, mT, BU and their mixtures. Potentials expressed in negative values ($-E$)

C_{pT} mol l^{-1}	$C_{\text{BU}}, \text{mol l}^{-1}$					C_{mT} mol l^{-1}	$C_{\text{BU}}, \text{mol l}^{-1}$				
	0	0.11	0.33	0.44	0.55		0	0.11	0.33	0.44	0.55
0	516.5	367.0	307.6	282.8	286.9	0	516.5	367.0	307.6	282.8	286.9
0.0015	590.8	470.2	378.3	357.8	346.5	0.0015	599.7	481.7	398.1	373.0	360.7
0.005	588.0	509.0	430.7	413.1	393.0	0.005	594.3	515.2	435.6	409.7	402.2
0.008	583.5	516.0	444.6	429.4	416.4	0.008	588.3	527.5	458.5	439.5	422.0
0.01	580.3	521.0	462.5	437.4	430.0	0.01	576.5	531.5	461.8	438.7	432.1
0.03	549.0	524.2	488.5	477.2	468.1	0.03	545.2	531.0	498.6	483.5	479.2
0.05	538.9	500.0	488.7	482.7	479.1	0.05	540.0	528.7	508.1	502.2	494.0

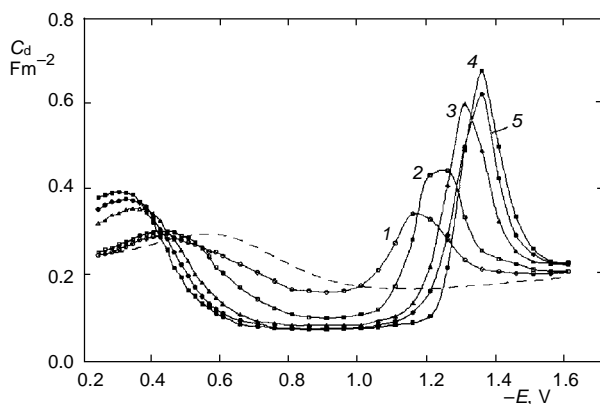


FIG. 1

Differential capacity curves of Hg in 1 mol l^{-1} $\text{NaClO}_4 + 0.008 \text{ mol l}^{-1}$ pT for different contents of BU: 1 $C_{\text{BU}} = 0$, 2 0.11, 3 0.33, 4 0.44, 5 0.55 mol l^{-1} . The dashed curve denotes the differential capacity of 1 mol l^{-1} NaClO_4

concentration increase of these isomers is accompanied by a shift of PZC towards positive potentials. The changes of PZC values in this case are much smaller than those for BU. In a mixture containing a constant amount of pT or mT small shift of the PZC with rising concentration of BU is observed. It decreases further for higher toluidine contents. This may indicate a predominant influence of toluidine on the formation of a mixed adsorption layer, despite the fact, that its concentration is much lower compared

TABLE II

Surface tension γ (mN m⁻¹) at PZC for pT, mT, BU and their mixtures

C_{pT} mol l ⁻¹	C_{BU} , mol l ⁻¹					C_{mT} mol l ⁻¹	C_{BU} , mol l ⁻¹				
	0	0.11	0.33	0.44	0.55		0	0.11	0.33	0.44	0.55
0	423.1	406.9	398.8	396.3	395.6	0	423.1	406.9	398.8	396.3	395.6
0.0015	423.7	411.8	401.2	396.8	393.1	0.0015	420.6	411.2	400.6	396.8	395.6
0.005	416.8	407.5	399.3	395.0	391.2	0.005	415.6	404.3	396.2	394.3	392.5
0.008	411.8	406.2	396.2	393.7	390.0	0.008	412.1	402.5	395.6	391.2	390.0
0.01	408.7	403.1	392.5	391.2	388.1	0.01	410.1	401.8	391.8	390.6	388.1
0.03	404.3	400.0	390.6	387.5	385.6	0.03	395.6	389.3	388.1	385.6	383.7
0.05	399.3	396.2	387.5	386.2	384.3	0.05	389.4	386.8	383.1	382.5	379.3

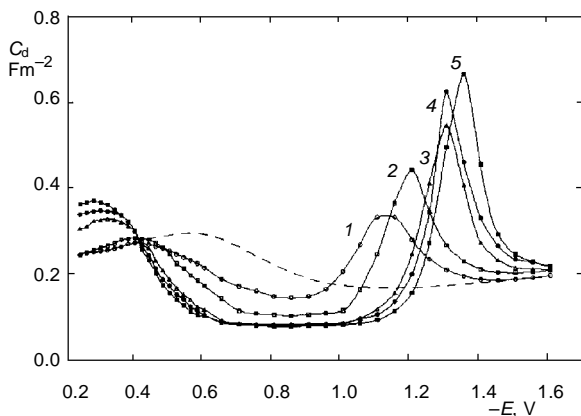


FIG. 2

Differential capacity curves of Hg in 1 mol l⁻¹ NaClO₄ + 0.008 mol l⁻¹ mT for different contents of BU, same as indicated in Fig. 1. The dashed curve denotes the differential capacity of 1 mol l⁻¹ NaClO₄

to that of BU. It should be stressed that the values of PZC for the two toluidine isomers are characteristic by their small differences.

Table II presents the values of surface tension γ at the PZC for pT, mT and BU solutions and for their mixtures. It can be seen that generally lower values of γ are obtained for mT than for pT. A predominance of the toluidine isomers in formation of the mixed adsorption layer is confirmed by the fact that for each BU concentration an addition of maximum 0.05 mol l^{-1} pT or mT causes a similar decrease of γ , as compared with the solution containing only BU. For lower concentrations of toluidine, the decrease of γ depends on BU concentration, which is the evidence for the existence of a mixed adsorption layer.

The value of differential capacity at PZC decreases with rising concentration of both BU and toluidine isomers due to the arrangement of the adsorption layer and due to the increase of its thickness²⁵. In the mixtures containing constant concentration of BU and increasing concentrations of pT or mT, similar changes of differential capacity take place as for individual substances but the obtained values are higher. The exceptions are the mixtures containing 0.11 mol l^{-1} BU and pT or mT where the values of differential capacity are higher than for toluidine but lower than for BU.

The values of surface excess Γ obtained for BU decrease monotonically with the potential. In the case of toluidine, however, the curves have a bell shape with the maxima at potentials close to the PZC. For the solutions containing BU and pT or mT mixtures (Figs 3 and 4) the curves are similar as for toluidine but with the maxima at potentials more negative than PZC. Such a shape of curves indicates competitive electrostatic interactions between organic molecules and water dipoles²⁶. The fact that

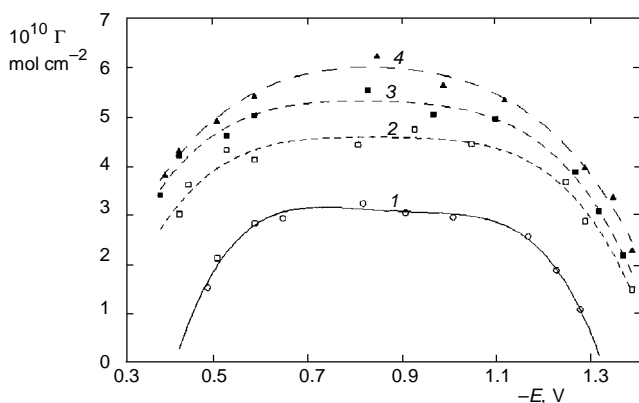


FIG. 3

The dependence of surface excess on potential for $1 \text{ mol l}^{-1} \text{ NaClO}_4 + 0.008 \text{ mol l}^{-1} \text{ pT}$ and different contents of BU: 1 $C_{\text{BU}} = 0.11$, 2 0.33 , 3 0.44 , 4 0.55 mol l^{-1}

the values of Γ for the BU–toluidine mixtures are much higher than for individual substances points to the synergetic character of adsorption.

Table III presents the values of Γ corresponding to the formal potentials E_0^f of Zn(II) reduction which confirms clearly the statement above. As follows from Table III, the values of Γ obtained for BU are much lower than those for toluidine and therefore at this potentials, toluidine adsorption is stronger than adsorption of BU. In the case of mT, the values of Γ are higher than those for pT.

TABLE III

Surface excess $\Gamma \cdot 10^{10}$ (mol cm⁻²) at E_0^f of the couple (Hg)Zn ($5 \cdot 10^{-3}$ mol l⁻¹)/Zn(II) ($5 \cdot 10^{-3}$ mol l⁻¹) in presence of pT, mT, BU and their mixtures

C_{pT} , mol l ⁻¹	C_{BU} , mol l ⁻¹					C_{mT} , mol l ⁻¹	C_{BU} , mol l ⁻¹				
	0	0.11	0.33	0.44	0.55		0	0.11	0.33	0.44	0.55
0	–	0.40	1.03	1.12	1.23	0	–	0.40	1.03	1.12	1.23
0.0015	0.35	2.68	4.20	4.73	5.20	0.0015	0.35	2.96	4.38	5.00	5.22
0.005	1.47	2.75	4.41	5.40	5.64	0.005	1.67	3.02	4.46	5.18	5.37
0.008	1.56	2.95	4.60	5.63	5.80	0.008	1.86	3.18	4.68	4.71	5.02
0.01	1.71	3.00	5.45	5.32	5.15	0.01	2.05	3.65	4.52	4.63	4.82
0.03	2.02	3.08	4.21	4.60	5.01	0.03	2.55	3.92	4.22	4.37	4.63
0.05	2.50	3.10	3.67	4.00	4.74	0.05	3.20	3.76	3.91	4.02	4.26

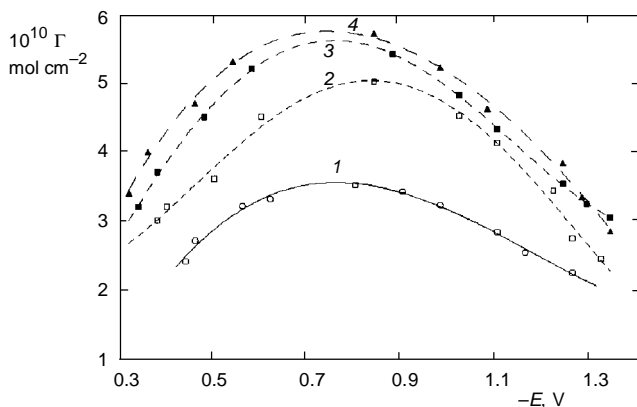


FIG. 4

The dependence of surface excess on potential for 1 mol l⁻¹ NaClO₄ + 0.008 mol l⁻¹ mT and different contents of BU, same as indicated in Fig. 3

The surface coverages θ for individual substances (at the formal potential E_0^f of Zn(II) ion reduction) are in the range from 0.087 to 0.267 for BU, assuming $\Gamma_m = 4.6 \cdot 10^{-10}$ mol cm $^{-2}$, which corresponds to a flat orientation of the molecules on the electrode surface²⁷. For pT the θ values are from 0.041 to 0.258 at $\Gamma_m = 9.7 \cdot 10^{-10}$ mol cm $^{-2}$ (ref.²⁸) and for mT from 0.037 to 0.340 at $\Gamma_m = 9.4 \cdot 10^{-10}$ mol cm $^{-2}$ (ref.²⁸). The values of Γ , obtained at higher concentrations for mixtures exceed the value of Γ_m for BU, but they are always lower than Γ_m for toluidine isomers.

Kinetics of Zn(II) Ion Reduction

The changes of DPP and SWV current peaks of Zn(II) ion reduction reflect the determined values of the standard rate constant k_s . Kinetic studies of Zn(II) ion reduction in presence of BU, toluidine isomers and their mixtures can be concluded in the following rules:

– Diffusion coefficients of Zn(II) reach the minimum value of $5.13 \cdot 10^{-6}$ cm 2 s $^{-1}$ in 0.05 mol l $^{-1}$ pT or mT solutions with 0.55 mol l $^{-1}$ BU.

– Reversible half-wave potentials $E_{1/2}^r$ change from -0.985 V to -0.995 V for pT and from -0.985 V to -1.003 V for mT. These slight changes indicate the formation of unstable Zn(II)–toluidine complexes. The stability of Zn(II)–mT complexes, however, seems to be slightly higher than with pT. The addition of BU into the solution causes always the changes of $E_{1/2}^r$ by a few mV.

– Difference between $E_{1/2}^r$ and E_0^f for Zn(II) reduction in 1 mol l $^{-1}$ NaClO $_4$ is -5 mV and it increases up to -9 mV in the 0.05 mol l $^{-1}$ solution of pT or mT mixture with of 0.55 mol l $^{-1}$ BU.

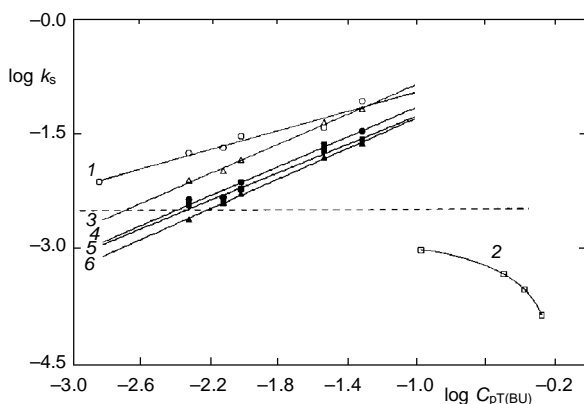


FIG. 5

Plots of $\log k_s$ vs $\log C_{pT}$ for (Hg)Zn ($5 \cdot 10^{-3}$ mol l $^{-1}$)/Zn(II) ($5 \cdot 10^{-3}$ mol l $^{-1}$) couple for different contents of BU: 1 $C_{BU} = 0$, 3 0.11, 4 0.33, 5 0.44, 6 0.55 mol l $^{-1}$ and $\log k_s$ vs $\log C_{BU}$ in absence of pT (2). The dashed line denotes $k_s = 3 \cdot 10^{-3}$ cm s $^{-1}$ for Zn(II) in 1 mol l $^{-1}$ NaClO $_4$

Figures 5 and 6 present a logarithmic dependence of the standard rate constant k_s of Zn(II) ion reduction on toluidine or BU concentration. The increase of pT concentration is accompanied by an increase of k_s from $3.31 \cdot 10^{-3} \text{ cm s}^{-1}$ to $8.29 \cdot 10^{-2} \text{ cm s}^{-1}$, while the maximum k_s value for mT is $2.76 \cdot 10^{-2} \text{ cm s}^{-1}$ (curve 1). An addition of BU into $1 \text{ mol l}^{-1} \text{ NaClO}_4$ changes the k_s value from $3.31 \cdot 10^{-3} \text{ cm s}^{-1}$ to $1.3 \cdot 10^{-4} \text{ cm s}^{-1}$ (curve 2). Greater accelerating activity of pT compared with mT is undoubtedly due to the formation of Zn(II)–toluidine complexes but not due to the toluidine adsorption because Γ values for pT are smaller compared to those for mT. The curves 3, 4, 5, 6 in Figs 5 and

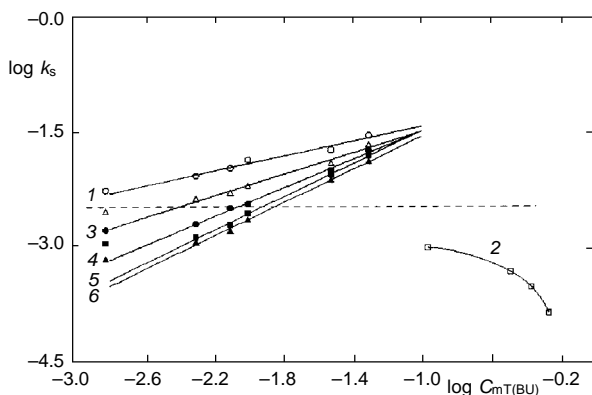


FIG. 6

Plots of $\log k_s$ vs $\log C_{mT}$ for the (Hg)Zn ($5 \cdot 10^{-3} \text{ mol l}^{-1}$)/Zn(II) ($5 \cdot 10^{-3} \text{ mol l}^{-1}$) couple for different contents of BU, same as indicated in Fig. 5

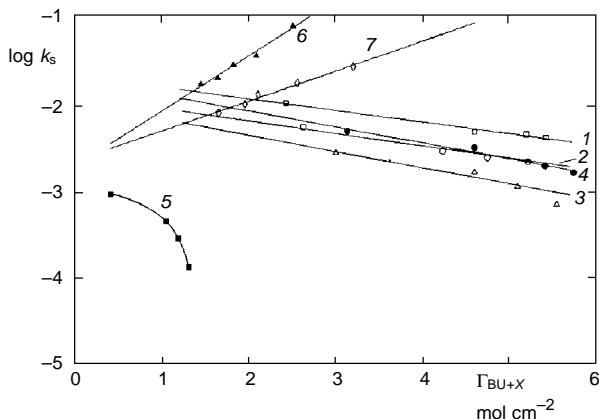


FIG. 7

Plots of $\log k_s$ for the (Hg)Zn ($5 \cdot 10^{-3} \text{ mol l}^{-1}$)/Zn(II) ($5 \cdot 10^{-3} \text{ mol l}^{-1}$) couple vs surface excess Γ_{BU+X} , where $X = mT$ or pT for different contents of pT: 1 $C_{pT} = 0.0015$, 2 0.008; of mT: 3 $C_{mT} = 0.015$, 4 0.008 mol l^{-1} ; 5 vs Γ_{BU} in absence of mT and pT, 6 vs Γ_{pT} and 7 vs Γ_{mT} in absence of BU

6 show the change of k_s with an increase of toluidine concentration at given BU concentration. It follows from the slope of the curves, that the BU concentration increase is accompanied by a faster increase of k_s , though the k_s values for the solution containing only toluidine are never reached. The analysis of the intersection of the straight lines 3, 4, 5, 6 with the dashed line corresponding to the k_s value of Zn(II) ion reduction in $1 \text{ mol l}^{-1} \text{ NaClO}_4$ in Figs 5 and 6 indicates that the compensation of inhibiting and accelerating effects takes place for the concentration ratio BU : pT \approx 85 and BU : mT \approx 35. This is an evidence for a greater accelerating effect of pT compared with mT. The dynamics of the acceleration–inhibition effect includes the changes of k_s in the range of 2.8 orders of magnitude with a symmetry in the relation to k_s values for Zn(II) ion reduction in $1 \text{ mol l}^{-1} \text{ NaClO}_4$.

Figure 7 represents the dependence of $\log k_s$ on $\Gamma_{\text{BU}+X}$ for chosen toluidine concentrations X and increasing BU concentration. The Γ values correspond to E_0^f of Zn(II) ion reduction. The slopes of the lines 1 and 2 for the determined pT concentrations are slightly lower than slopes of lines 3 and 4 obtained for mT. It confirms a higher effectivity of pT compared with mT to eliminate the inhibiting effect of BU. The straight lines corresponding to one toluidine isomer are parallel within certain range of concentrations. It indicates that the accessibility of BU molecules for the electrode surface is proportional to the toluidine concentration and the interaction forces have steady character. This can be explained also by a similar character of adsorption isotherms.

CONCLUSIONS

The study of inhibition and acceleration effects on the reduction of Zn(II) ion provides an insight into the toluidine isomer–BU adsorption equilibria on the mercury electrode surface.

The PZC and corresponding γ values show that the toluidine isomers predominate in the mixed adsorption layer in the concentration ratio 1 : 10 + 1 : 100.

The total surface excesses calculated for the BU–toluidine mixtures are higher than the sum of Γ corresponding to individual substances which show the synergetic character of the BU–toluidine coadsorption.

The bell-shape of the curves $\Gamma = f(E)$ for the toluidine isomers and the BU–toluidine mixture is the evidence of toluidine–H₂O or toluidine–BU–H₂O electrostatic interactions in the adsorption layer.

The dependence of Γ on concentration of toluidine for BU–toluidine mixture at E_0^f of Zn(II) reduction and constant concentration of BU yields maximum. Here Γ increases initially with rising concentration of toluidine confirming the rise of toluidine adsorption (k_s values also grow). Then the decrease of Γ is observed with the further increase of k_s . This may suggest that BU molecules are displaced from the electrode surface with rising toluidine concentration.

From the k_s values can be assumed that the compensation of acceleration and inhibition effects of Zn(II) ion reduction occurs in the studied concentration range with the molar concentration ratio of BU : pT \approx 85 and BU : mT \approx 35. The studies presented in this paper thus brings up the new informations concerning formation and properties of the mixed adsorption layers beyond the area of maximum adsorption.

The author thanks Professor K. Sykut for valuable discussions.

REFERENCES

1. Nesterenko A. F., Bachtiarow N. G., Fastowiec W. W., Jamnowa T. P., Loszkariew M. A.: *Elektrokhimiya* 23, 1623 (1987).
2. Tedoradze G. A., Arakielan R. A., Bielokos E. D.: *Elektrokhimiya* 2, 563 (1966).
3. Muraszewicz E. W., Afanasewa L. F., Bachtiarow N. G., Nesterenko A. F., Loszkariew M. A.: *Elektrokhimiya* 22, 1308 (1986).
4. Rodriguez-Amaro R., Munoz E., Ruiz J. J., Avila J. L., Camacho L.: *J. Electroanal. Chem.* 358, 127 (1993).
5. Munoz E., Rodriguez-Amaro R., Ruiz J. J., Avila J. L., Camacho L.: *J. Electroanal. Chem.* 324, 359 (1992).
6. Batina N., Cosovic B.: *J. Electroanal. Chem.* 227, 129 (1987).
7. Sykut K., Saba J., Marczevska B., Dalmata G.: *J. Electroanal. Chem.* 178, 295 (1984).
8. Sykut K., Dalmata G., Marczevska B., Saba J.: *Pol. J. Chem.* 65, 2241 (1991).
9. Sykut K., Dalmata G., Nowicka B., Saba J.: *Anal. Chim. Acta* 118, 369 (1980).
10. Sykut K., Dalmata G., Saba J., Marczevska B.: *Chem. Anal.* 36, 1 (1991).
11. Sykut K., Dalmata G., Saba J., Kujawa M.: *Ann. UMCS* 42, 51 (1987/88).
12. Saba J.: *Electrochim. Acta* 39, 711 (1994).
13. Saba J.: *Pol. J. Chem.* 67, 703 (1993).
14. Moncelli R. M., Foresti M. L., Guidelli R.: *J. Electroanal. Chem.* 295, 225 (1990).
15. Damaskin B. B., Survila A. A., Rybalka L. E.: *Elektrokhimiya* 3, 146 (1967).
16. Borowaya N. A., Damaskin B. B.: *Elektrokhimiya* 8, 1529 (1972).
17. Schiffrin D. J.: *J. Electroanal. Chem.* 23, 168 (1969).
18. Parsons R.: *Trans. Faraday Soc.* 51, 1518 (1955).
19. Ilkovic D.: *Collect. Czech. Chem. Commun.* 6, 498 (1934).
20. Turnham D. S.: *J. Electroanal. Chem.* 10, 19 (1965).
21. Furman N. S., Cooper W. Ch.: *J. Am. Chem. Soc.* 72, 5667 (1950).
22. Galus Z.: *Elektroanalityczne metody wyznaczania stalych fizykochemicznych*, p. 250. PWN, Warszawa 1979.
23. Sluyters J. H., Oomen J. J. C.: *Rec. Trav. Chim.* 79, 1101 (1960).
24. Sluyters J. H.: *Rec. Trav. Chim.* 29, 1092 (1960).
25. Mielniczenko J. A., Burikina W. C., Seczin L. G., Panacenko S. A., Nesterenko A. F., Loszkariew M. A.: *Elektrokhimiya* 23, 762 (1987).
26. Schapink F. W., Oudeman M., Leu K. W., Helle J. N.: *Trans. Faraday Soc.* 56, 415 (1960).
27. Blomgren E., O'M. Bockris J., Jesch C.: *J. Phys. Chem.* 65, 2000 (1961).
28. Joshi K. M., Mahajan S. J., Bapat M. R.: *J. Electroanal. Chem.* 54, 371 (1974).